SUPPLEMENTARY INFORMATION SCALING OF TROPICAL-CYCLONE DISSIPATION

ÁLVARO CORRAL AND ALBERT OSSÓ, JOSEP ENRIC LLEBOT

1. SUPPLEMENTARY METHODS

1.1. **Summary of the Analysis.** A sketch of our procedure is shown in Fig. S1. For a single tropical cyclone, the *PDI*, which is an estimation of dissipated energy, is calculated as the sum of the cube of the velocity profile. When this is done for many tropical cyclones, a probability distribution for the *PDI* emerges. This distribution can also be filtered by different climatic variables, in order to evaluate the characteristics of the dissipation of energy as a function of those variables.

1.2. **Data.** As it is mentioned in the main text, the tropical-cyclone data used in the research has been obtained from the best tracks provided by the NOAA's National Hurricane Center (NHC) [1, 2], for the North Atlantic (N. Atl.) and the Northeastern Pacific (E. Pac.); and by the US Navy's Joint Typhoon Warning Center (JTWC) [3, 4], for the Northwestern Pacific (W. Pac.) and the Southern Hemisphere (S. Hem.). A remarkable difference between the databases of both agencies is that the one from the JTWC includes a few tropical depressions each year, whereas the records from the NHC exclude such small storms.

Figure S2 shows the longitude and latitude of the best tracks of all tropical cyclones analyzed, in addition to those corresponding to the North Indian ocean (N. Ind.), which have not been considered in the paper due to their poor statistics. Note that there is not a clear boundary between the Northwestern and Northeastern Pacific basins, as well as between the Southern Indian and Southwestern Pacific. For this reason we have analyzed the basins as provided in the records of each agency.

1.3. **Probability Density.** In order to obtain the distribution of the tropical-cyclone *PDI*s we use the probability density, defined as the probability that the value of the power dissipation index is in a narrow interval, $[PDI, PDI + dPDI)$, divided by the size of the interval, $dPDI$. Mathematically,

$$D(PDI) \equiv \frac{\text{Prob}[PDI \leq \text{value} < PDI + dPDI]}{dPDI},$$

and the probability is estimated as the number of occurrences $n(PDI)$ in a given interval divided by the total number of occurrences, N, i.e.,

$$D(PDI)dPDI \simeq \frac{n(PDI)}{N}.$$

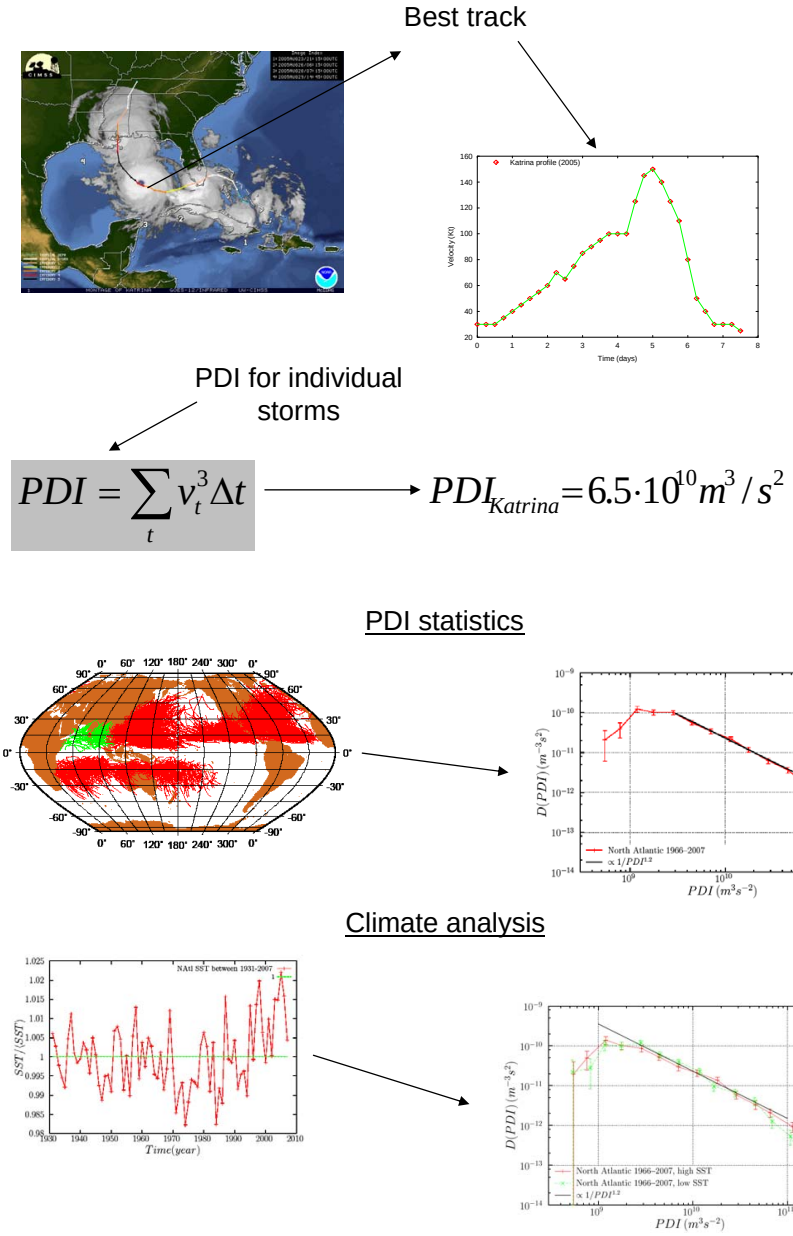

FIGURE 1. Outline of the procedure used in the paper. Hurricane Katrina is selected as an illustration of the calculation of the *PDI*. The large-scale application of the same calculation yields the *PDI* probability density, as the North Atlantic case shows. Separating years of high and low sea surface temperature, for example, splits the probability density into two contributions, shown here for the North Atlantic as well.

CRM Preprint Series number 1073

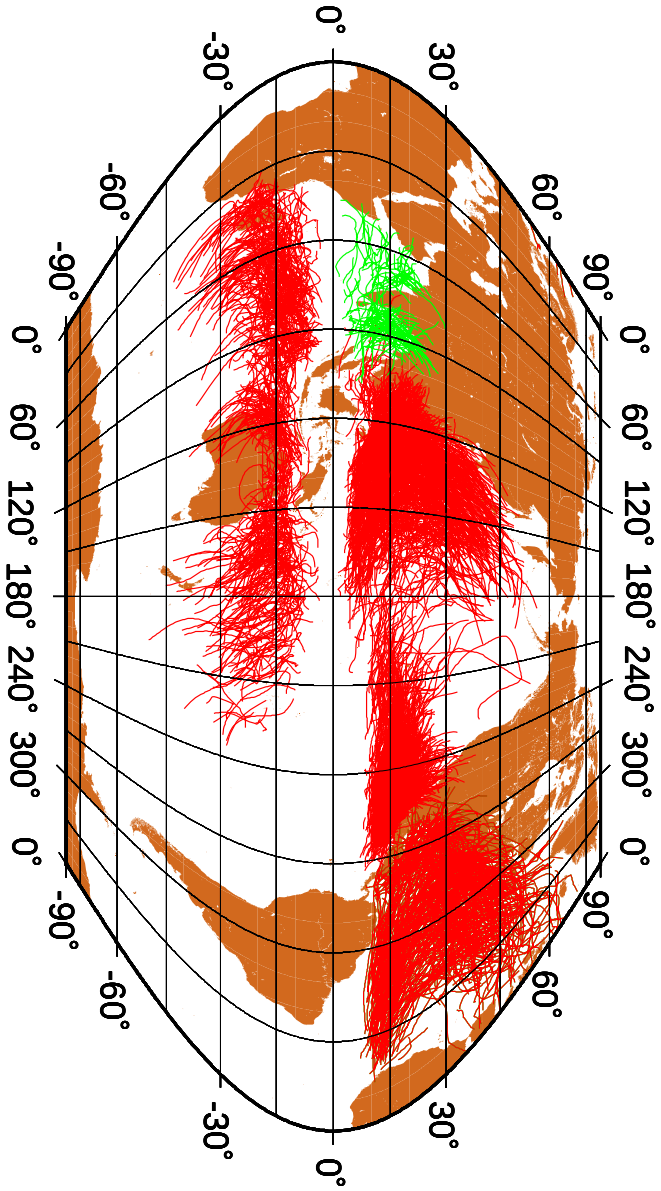

FIGURE 2. Worldwide tropical-cyclone activity analyzed in the main text. The North Atlantic and Northeastern Pacific basins include all recorded hurricanes and tropical storms from 1966 to 2007, the rest of the basins are restricted to tropical cyclones from 1986 to 2007, including also some tropical depressions. The Southern Hemisphere record ends in May 2007. The number of tropical cyclones in each basin is: N. Atl., 469; E. Pac., 674; W. Pac., 690; S. Hem., 601; N. Ind., 110. North Indian TCs, excluded from the analysis, are plotted in a different colour.

CRM Preprint Series number 1073

For variables distributed across a wide range of scales, it is convenient to take a variable size of the interval, increasing accordingly to the scale of the variable. The most natural selection is what is called logarithmic binning [5], where each interval is a factor c larger than the previous one, i.e., $[PDI_{min}, PDI_{max}) = [m, cm)$, $[cm, c^2m)$, $[c^2m, c^3m)$, etc.; so, for the $k-$th interval, $dPDI = c^{k-1}(c-1)m$. We have usually taken $c = \sqrt[5]{10} \simeq 1.58$, which corresponds to 5 intervals per decade, and an absolute minimum value, for instance, $m = 10^8$ m^{3}s^{-2}.

In this way, the value of $D(PDI)$ is associated to the whole interval $PDI_{min} = c^{k-1}m \leq PDI < PDI_{max} = c^k$, as in a bar histogram. If we want to take a single point of the interval, PDI^*, to be representative of the probability density, we need to solve the equation $D(PDI^*) = [F(PDI_{max}) - F(PDI_{min})]/dPDI$, where $F(PDI)$ is the cumulative distribution function, $F(PDI) \equiv \int_0^{PDI} D(x)dx$. Note that the equation depends on the mathematical form of the distribution. However, a prescription for PDI^* is given in Ref. [5], which shows that the geometric mean of the limits of the interval is a reasonable solution, i.e., $PDI^* = \sqrt{PDI_{min}PDI_{max}}$. Nevertheless, as it is explained in the next subsection, our estimates of the power-law exponent are independent on the estimation of the probability densities, which are only displayed as a visual indication.

The error bars for each interval are estimated from the standard deviation of the density, obtained from the formula

$$\varepsilon(PDI) = \varepsilon_{rel}(PDI)D(PDI)$$

with

$$\varepsilon_{rel}(PDI) = \sqrt{\frac{1-P}{n}} \simeq \frac{1}{\sqrt{n}},$$

which makes use of the binomial distribution for the number of counts, with $P \equiv n/N = D(PDI)dPDI$, see for instance page 185 of Ref. [6].

1.4. **Power-law Fit and Kolmogorov-Smirnov Goodness-of-Fit Test.** In order to fit the *PDI* distributions and to test the goodness of such fits we essentially follow the method proposed by Clauset *et al.* [7], generalizing it for the case in which the power law has both a lower and an upper cutoff, A and B, respectively.

The power-law exponent is obtained by maximizing the likelihood function, or equivalently, its logarithm, the log-likelihood. The normalized density, with $x \equiv PDI$ and defined between $x = A$ and $x = B$, is

$$D(x) = \frac{C}{x^\alpha} = \frac{(\alpha-1)A^{\alpha-1}}{1-r^{\alpha-1}}\frac{1}{x^\alpha}$$

with $r \equiv A/B$. The log-likelihood $\mathscr{L}$ is defined, dividing by the number of data N_{AB} in the range $A \leq x \leq B$, as

$$\mathscr{L}(\alpha) = \frac{1}{N_{AB}}\sum_{i=1}^{N_{AB}} \ln D(x_i) = \ln\frac{\alpha-1}{1-r^{\alpha-1}} - \alpha\ln\frac{G}{A} - \ln A,$$

where i labels the different data points (the tropical cyclones considered) inside the interval $[A,B]$ and G is the geometric mean of the data in the considered range, i.e., $\ln G = \sum_i \ln x_i / N_{AB}$. The log-likelihood only depends on one unknown parameter, α, as, following Clauset *et al.*, A and B (and therefore r) are taken as fixed parameters (later they will be allowed to vary). Maximization of the log-likelihood is performed numerically to obtain the maximum-likelihood estimator for α, which we call here α_{data} (for details in the procedure, see Ref. [8]). The uncertainty of the exponent α_{data} can be obtained from its standard deviation, σ_α; we have used the value derived by Aban *et al.* [9].

Usually, at this point, provided a fitting range and the estimated parameters, the Kolmogorov-Smirnov (KS) test [10] (or an equivalent test) quantifies the goodness of the fit. However, Clauset *et al.* use the KS statistic to decide the best fitting range, which for them is the one that minimizes the KS statistic. Let us recall that the KS statistic, or KS distance, is defined as

$$d_{data} \equiv \max_{A \le x \le B} [F_{data}(x) - F(x|\alpha_{data})],$$

where $F(x|\alpha_{data})$ is the theoretical power-law distribution (stressing the dependence of the distribution on its parameter, with value α_{data}), $F(x|\alpha_{data}) \equiv \int_A^x D(x|\alpha_{data})dx = C(1/A^{\alpha_{data}-1} - 1/x^{\alpha_{data}-1})/(\alpha_{data}-1)$, and $F_{data}(x)$ is the empirical cumulative distribution of the data, calculated simply as the fraction of data below a given value x, which results in a staircase-like function.

In contrast with Clauset *et al.*'s case, where $B \to \infty$, when B is finite several power laws can fit different portions of the distribution. We just chose the values of A and B that minimize d_{data} under the constrain that B/A has to be large enough, typically $B/A > 20$. This yields the optimal values $\hat{A}$ and $\hat{B}$, with a corresponding maximum-likelihood exponent $\hat{\alpha}_{data}$ and the minimized KS statistic $\hat{d}_{data} = \min_{\forall A,B \text{ s.t. } B/A>20}[d_{data}]$.

Once we have decided a fitting range (i.e., $\hat{A}$ and $\hat{B}$) and have also the corresponding exponent $\hat{\alpha}_{data}$, we need to quantify the goodness of the fit. The temptation is just to use the KS tables, however, as the distribution that we are going to test is the optimum one that fits the data, we cannot use this procedure. In order to avoid such a bias, the alternative is to compute the distribution of the KS statistic by Monte Carlo simulations [7]. The key point is to proceed with the simulated data exactly in the same way as with the empirical data, avoiding in this way any bias.

To be concrete, our null hypothesis states that, for $\hat{A} \le x \le \hat{B}$, the data come from the power-law distribution $F(x|\hat{\alpha}_{data})$ (i.e., $D(x|\hat{\alpha}_{data})$, where the dependence on $\hat{A}$ and $\hat{B}$ is implicit). Therefore, we need to simulate N data, following such distribution between $\hat{A}$ and $\hat{B}$ but with a distribution similar to the empirical one outside this range, in order to be able to apply to the simulated data the same estimation procedure used for the empirical data. We generalize the semiparametric method described in Ref. [7], in such a way that the simulated values outside the interval $[\hat{A},\hat{B}]$ are randomly selected from the empirical data and the values inside the interval are taken from a synthetic

power-law distribution. Let us define $\hat{N}_A$ as the number of data with $x < \hat{A}$, $\hat{N}_{AB}$ as the number of data with $\hat{A} \leq x \leq \hat{B}$, and $\hat{N}_B$ as the number of data with $x > \hat{B}$, fulfilling $N = \hat{N}_A + \hat{N}_{AB} + \hat{N}_B$. So, with probability $\hat{N}_A/N$ we take at random one of the empirical data with $x < \hat{A}$, with probability $\hat{N}_B/N$ we take at random one of the empirical data with $x > \hat{B}$ and with probability $\hat{N}_{AB}/N$ we generate a power-law random number as

$$x = \frac{\hat{A}}{\left[1 - (1 - \hat{r}^{\hat{\alpha}_{data}-1})u\right]^{1/(\hat{\alpha}_{data}-1)}},$$

where $\hat{r} \equiv \hat{A}/\hat{B}$ and u is uniformly distributed between 0 and 1.

In this way, we select arbitrary values of A and B and fit the exponent α in the corresponding interval by maximum likelihood to the simulated data, as before, obtaining an estimator α_{sim}; then we compute the KS statistic as

$$d_{sim} \equiv \max_{A \leq x \leq B} [F_{sim}(x|\hat{\alpha}_{data}) - F(x|\alpha_{sim})],$$

where $F_{sim}(x|\hat{\alpha}_{data})$ is the cumulative distribution of the simulated data, and $F(x|\alpha_{sim})$ is the theoretical distribution for such simulated data, with the parameter α_{sim} obtained from maximum likelihood from the simulated data. As before, we select the fitting range for which A and B yield $\hat{d}_{sim} \equiv \min[d_{sim}]$, with the condition that $B/A > 20$, which leads to the values $\hat{A}_{sim}$, $\hat{B}_{sim}$, $\hat{\alpha}_{sim}$ and, our main interest, $\hat{d}_{sim}$.

Repeating this Monte Carlo procedure many times we will obtain the distribution of the KS statistic $\hat{d}_{sim}$ under the null hypothesis, i.e., for data following the distribution $F(x|\hat{\alpha}_{data})$. In particular, the $p-$value, defined as

$$p \equiv \text{Prob [KS statistic takes value larger than the empirical value if the null hypothesis is true]},$$

is estimated as

$$p = \frac{\text{Number of simulations with } \hat{d}_{sim} \geq \hat{d}_{data}}{\text{Total number of simulations}}.$$

In general, it is straightforward to see that, under the null hypothesis, the $p-$value itself will be randomly distributed, with a uniform distribution defined between 0 and 1. It seems clear that if $p = 0.9$, $p = 0.5$ or even $p = 0.2$, we should not reject the null hypothesis, whereas if $p = 0.0001$ we must reject it. Intermediate cases are more delicate. In any case, if we reject the null hypothesis, the $p-$value gives us the probability that we are rejecting a true null hypothesis.

Finally, the uncertainty of the $p-$value, which we call σ_p is obviously associated to the number of simulations used to obtain it. The number of simulations with KS statistic larger than $\hat{d}_{data}$ is a binomial variable. Using the same argument than for the error bars of the probability density (see Ref. [6]) one gets that $\sigma_p/p \simeq \sqrt{(1-p)/(pN_s)}$, where N_s denotes here the total number of simulations, and therefore $\sigma_p \simeq \sqrt{p(1-p)/N_s}$. Note that for $p \simeq 0.5$ and $N_s \simeq 2500$, σ_p is around 0.01,

in agreement with the recipe given in Ref. [7]; however, if p is close to 0 or 1, this agreement is not valid anymore.

Section II contains the results of applying this procedure to the tropical-cyclone *PDI*s.

1.5. **Kolmogorov-Smirnov test for similarity of distributions.** We can also test if two data sets come from the same distribution, independently on the shape of the distribution, using the two-sample Kolmogorov-Smirnov test [10]. In this case the KS statistics is defined as

$$d \equiv \max_{\forall x}[F_{data\,1}(x) - F_{data\,2}(x)],$$

where $F_{data\,1}(x)$ and $F_{data\,2}(x)$ refer to the empirical cumulative distributions of the two data sets under consideration. The distribution of d can be easily calculated with the help of some numerical recipes, given only the number of data in each set [10]. In this way we can test both the stationarity of the distributions of *PDI* and their dependence with *SST* and *MEI*. The results for the tropical-cyclone data are provided in the next section.

basin	period	N	$A\,(\mathrm{m}^3/\mathrm{s}^2)$	$B\,(\mathrm{m}^3/\mathrm{s}^2)$	N_{AB}	CN_{AB}/N	$\alpha \pm \sigma_\alpha$	d_{data}	$p-$value
N. Atl.	1966-2007	469	$2.7\cdot10^9$	$6.3\cdot10^{10}$	328	37.423	1.190± 0.060	$2.40\cdot10^{-2}$	69.0 ± 1.5 %
E. Pac.	1966-2007	674	$3.2\cdot10^9$	$7.4\cdot10^{10}$	450	28.456	1.175± 0.050	$1.56\cdot10^{-2}$	98.4 ± 0.4 %
W. Pac.	1986-2007	690	$0.5\cdot10^9$	$14.7\cdot10^{10}$	655	0.073	0.960± 0.025	$1.81\cdot10^{-2}$	58.8 ± 1.6 %
S. Hem.	1986-2007	601	$1.6\cdot10^9$	$9.3\cdot10^{10}$	474	3.593	1.110± 0.040	$2.35\cdot10^{-2}$	24.0 ± 1.3 %
N. Atl.	1900-1953	436	$1.8\cdot10^9$	$9.3\cdot10^{10}$	381	2.299	1.090 ± 0.050	$2.93\cdot10^{-2}$	19.1 ± 1.2 %
N. Atl.	1954-2007	579	$2.2\cdot10^9$	$7.9\cdot10^{10}$	446	18.320	1.170 ± 0.050	$2.02\cdot10^{-2}$	76.2 ± 1.3 %

TABLE 1. Parameters of the maximum likelihood estimation and the KS test for the *PDI* data in Figs. 1(a) and 1(b) (upper and lower part of the table, respectively). N_{AB} refers to the number of tropical cyclones with *PDI* value between A and B; CN_{AB}/N is the constant of the power law that fits the distribution between A and B when it is normalized from 0 to ∞, its units are $(\mathrm{m}^3/\mathrm{s}^2)^{\alpha-1}$. Note that in the worst case, one standard-deviation uncertainty is around ±0.06. A and B are determined with a resolution of 30 points per decade. The $p-$values are calculated from 1000 Monte Carlo simulations.

2. SUPPLEMENTARY RESULTS

2.1. **Power-law distribution of tropical-cyclone dissipation.** Table S1 shows the results of applying the procedure to determine the fitting range and the power-law exponent (explained in the previous section) to the *PDI* data sets of Fig. 1(a). It is apparent that the proposed fitting power-law distributions cannot be rejected, as the $p-$values are high enough. In fact, one of the values (E. Pac.) is very close to 1; this would mean that the power-law fit is "too good", which could be a consequence of the fact that the statistical independence of the variables does not hold. We note that correlations between the size of successive occurrences of natural hazards have become an important research topic recently [6, 11, 12]. In any case, the tropical-cyclone-*PDI* power-law behaviour is very clear over the selected range.

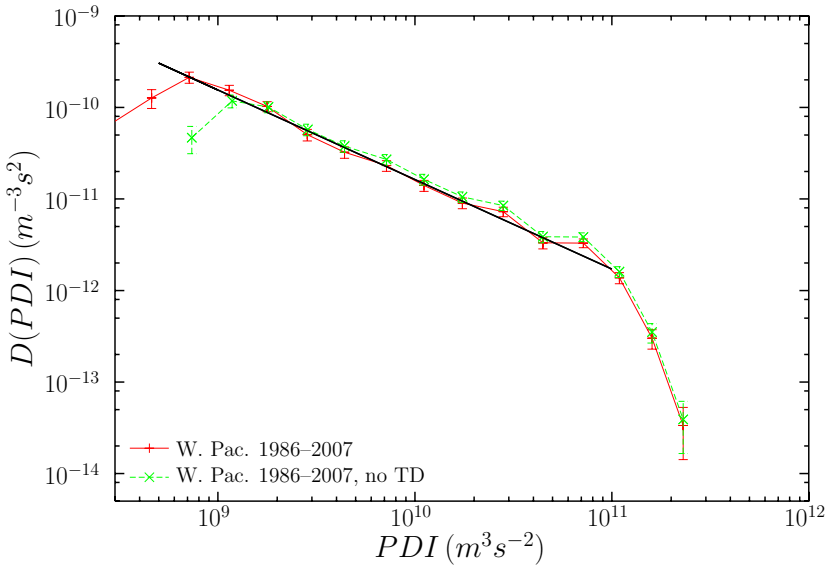

FIGURE 3. Comparison of *PDI* probability densities in the Northwestern Pacific excluding tropical depressions (TD) and including them (as in the main text).

2.2. **Effect of tropical depression incompleteness.** As we have already mentioned, records for the Northwestern Pacific and the Southern Hemisphere, compiled by the JTWC, contain some tropical depressions, whereas the Northeastern Pacific and the Northern Atlantic data are devoid of these storms (defined by maximum sustained surface velocities below 32 knots). The inclusion of tropical depressions enlarges the range of the power-law behaviour to small values of *PDI*, as can be seen in Fig. S3. So, we can attribute to this the fact that the power-law range is shorter in the Northeastern Pacific and the Northern Atlantic. In the same way, as only tropical depressions of

some significance are retained in the records, we expect that the addition of not significant tropical depressions would extend further the power-law range to smaller values of the *PDI*.

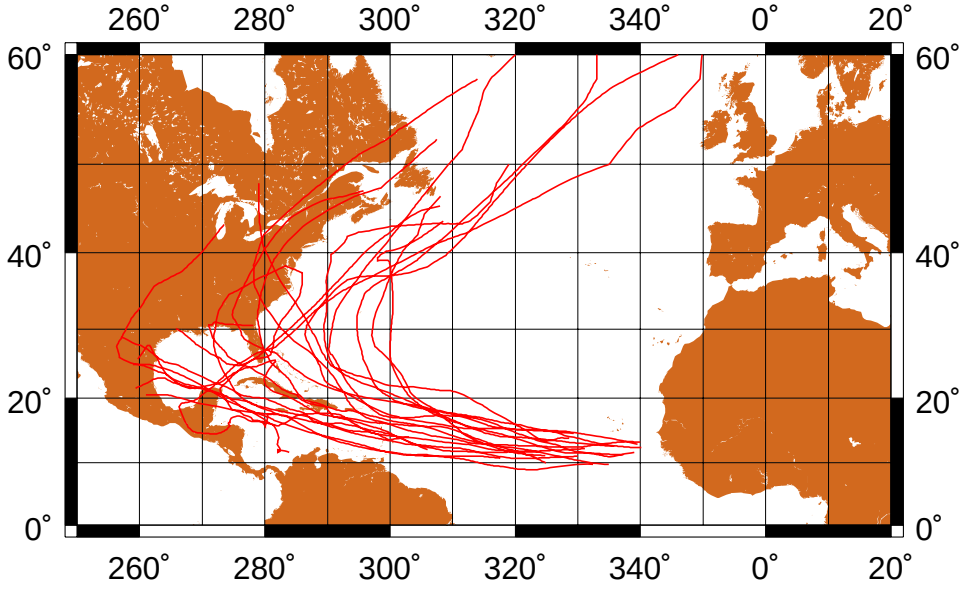

FIGURE 4. Tropical-cyclone best tracks with *PDI* greater than $10^{11}\,\mathrm{m^3 s^{-2}}$ for the North Atlantic, during the period 1966-2007.

2.3. **Effect of the Finite Size of the Basin.** Figures S4, S5 and S6 show the best tracks of the tropical cyclones with *PDI* values in the tail of the distribution, concretely, $PDI > 10^{11}\,\mathrm{m^3/s^2}$, except for the Northwestern Pacific, where we have taken $PDI > 1.5 \cdot 10^{11}\,\mathrm{m^3/s^2}$ (due to the large number of cyclones which verify the former condition). It is clear that, in general, these storms travel through the whole basin, being limited in their evolution by the finiteness of the size of the basins.

We can make this argument quantitative. Below we count how many of these large-in-*PDI* tropical cyclones end by effect of becoming extratropical, landfall, or other factors. Note that the information contained in the records is not fully reliable in this regard, and we have needed to consult other sources (among them [13, 14, 15]). The results are:

- North Atlantic
  - Extratropicals: 12 (Faith 1966, David 1979, Gilbert 1988, Hugo 1989, Luis 1995, Edouard 1996, Mitch 1998, Gert 1999, Fabian 2003, Isabel 2003, Frances 2004, Wilma 2005).
  - Landfall: 7 (Inez 1966, Beulah 1967, Allen 1980, Georges 1998, Ivan 2004, Emily 2005, Dean 2007).
  - Other: 1 (Gabrielle 1989).

CRM Preprint Series number 1073

- Northeastern Pacific
  - Extratropicals: 5 (Fico 1978, Kevin 1991, John 1994, Guillermo 1997, Ioke 2006).
  - Landfall: 2 (Norbert 1984, Oliwa 1997).
  - Other: 7 (Uleki 1988, Trudy 1990, Tina 1992, Emilia 1994, Linda 1997, Paka 1997, Dora 1999).
- Northwestern Pacific
  - Extratropicals: 7 (Mireille 1991, Yvette 1992, Yates 1996, Joan 1997, Keith 1997, Lupit 2003, Chaba 2004).
  - Landfall: 0.
  - Other: 4 (Gay 1992, Angela 1995, Paka 1997, Fengshen 2002).
- Southern Hemisphere
  - Extratropicals: 6 (Harry 1989, Hanitra 1989, Susan 1997-98, Frank 2004, Olaf 2005, Percy 2005).
  - Landfall: 7 (Alibera 1989-90, Geralda 1994, Litanne 1994, Hudah 2000, Fay 2004, Ingrid 2005, Monica 2006).
  - Absorbed: 1 (Ron 1998 by Susan).
  - Other: 7 (Rewa 1993-94, Daryl/Agnielle 1995, Melanie/Bellamire 1996, Pancho/Helinda 1997, Dina 2002, Hary 2002, Kalunde 2003).

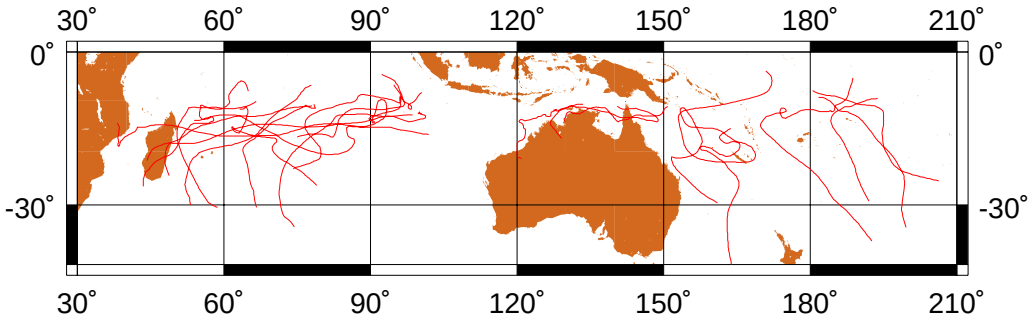

FIGURE 5. Tropical-cyclone best tracks with *PDI* greater than $10^{11}\,\mathrm{m^3 s^{-2}}$ for the Southern Hemisphere, during the period 1986-2007 (ending in May). Note that for such large storms the Southern Indian and the Southern Pacific basins get clearly separated; nevertheless, the similar sizes of both basins justifies their treatment as a unique system, in order to improve the statistics.

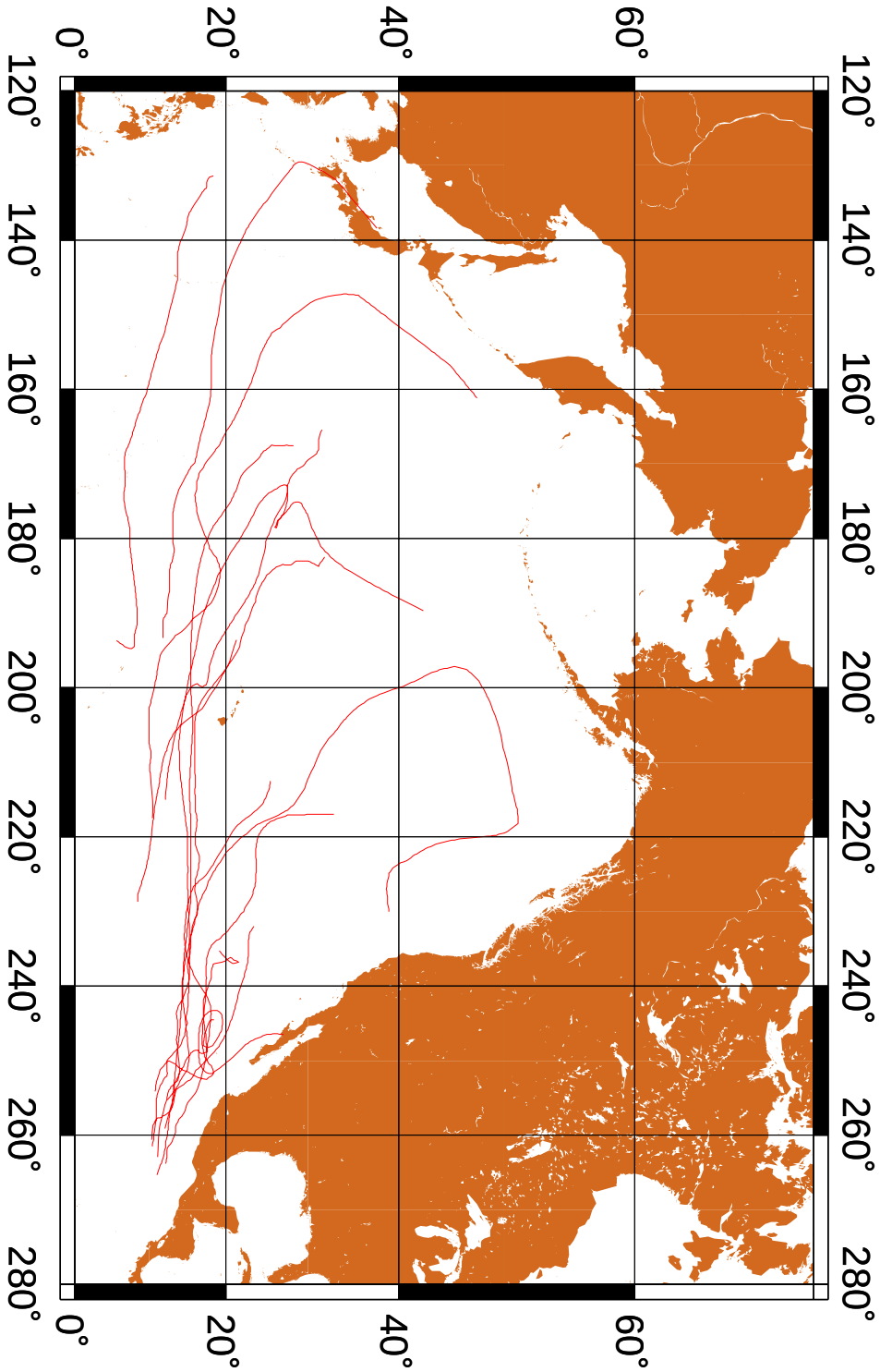

CRM Preprint Series number 1073

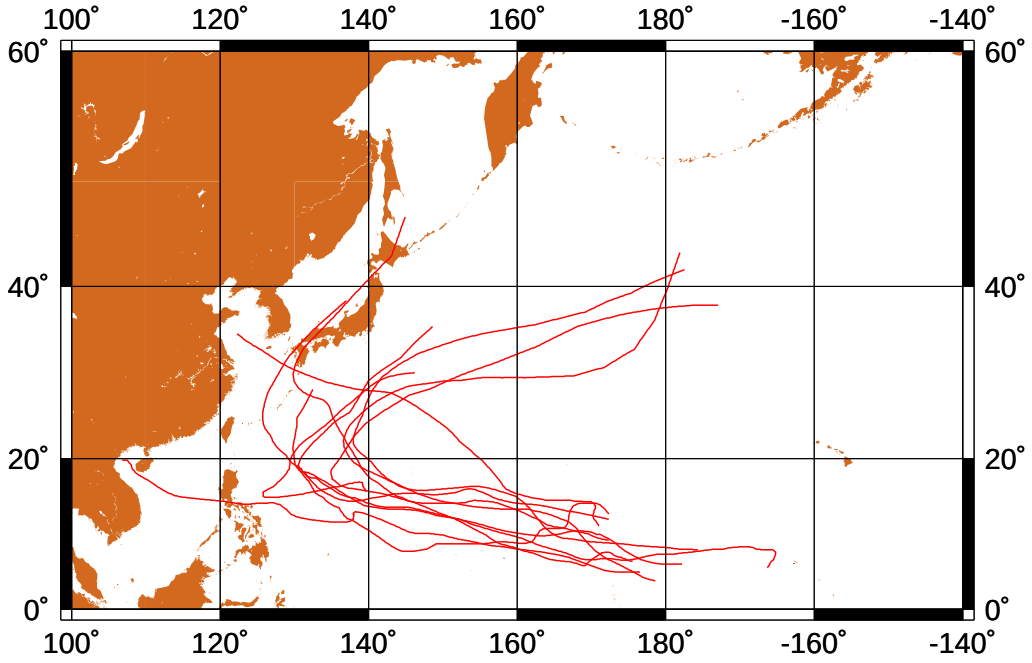

FIGURE 6. Tropical-cyclone best tracks with *PDI* greater than $10^{11}\,\mathrm{m^3 s^{-2}}$ for the Northeastern Pacific during the period 1966-2007 and greater than $1.5\cdot 10^{11}\,\mathrm{m^3 s^{-2}}$ for the Northwestern Pacific during 1986-2007. Note that some storms cross the "boundary" between the basins and there is one storm that is present in both databases.

We see how in all basins, except in the Northeastern Pacific, most of the largest (in *PDI*) tropical cyclones end by transitioning into extratropical cyclones or by landfall. In both cases this constitutes a boundary or finite size effect. In the Northeastern Pacific these termination mechanisms take place in about half of the largest-in-*PDI* hurricanes. But this does not exclude that for some of the hurricanes in the other half of the record a boundary effect is also playing a role; indeed, hurricanes at somehow low latitudes encounter soon the cold California Current to the North, and also cool *SST* to the West. This effectively delimits the lifetime of hurricanes and therefore the size of the basin.

A finite-size analysis can be easily performed. We restrict the calculation of *PDI*s only to the cases in which the best-track coordinates are in some bounded region of the basin. Mathematically,

$$PDI \equiv \sum_{t \text{ s.t. } (x,y)\in R} v_t^3 \Delta t,$$

which is restricted to the case (time) in which the coordinates (x,y) are inside region R. In order keep the statistics as high as possible, we will average the *PDI* distributions over regions R with the same size.

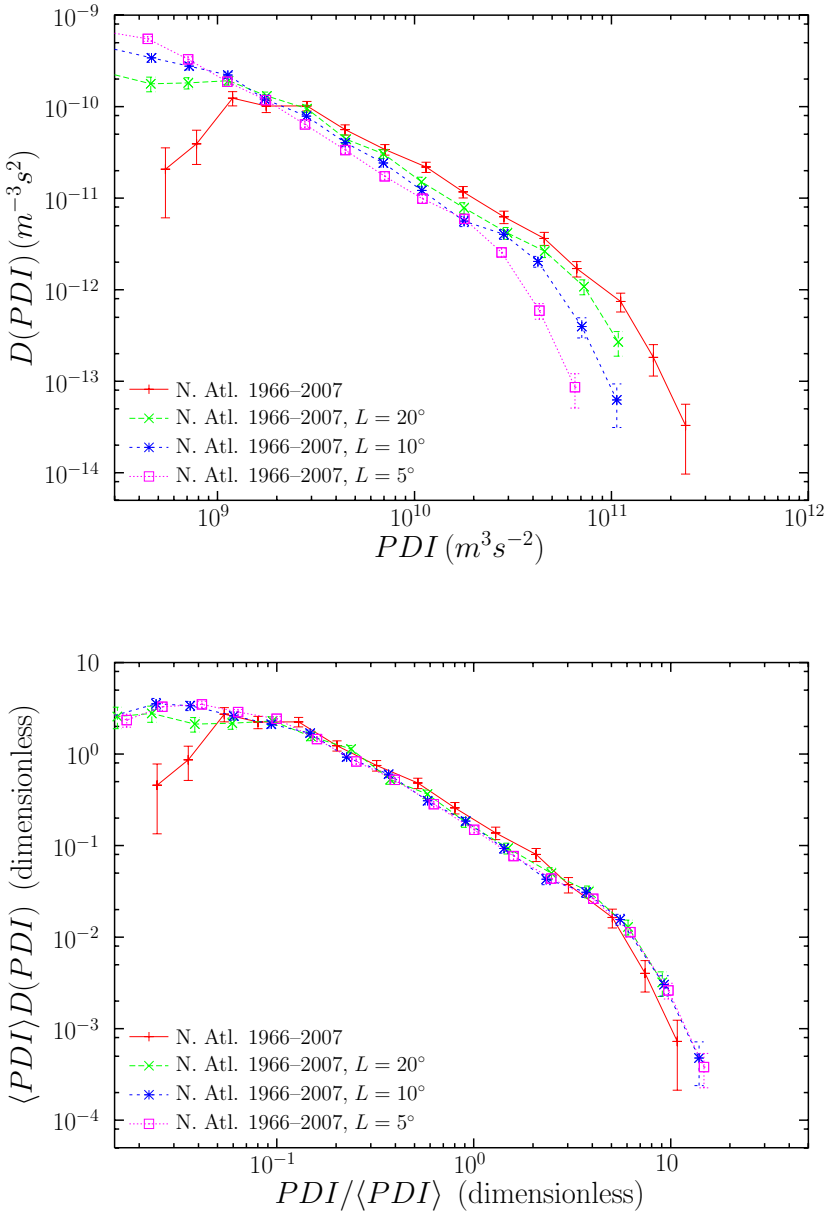

FIGURE 7. (a) *PDI* probability densities averaged over sections of different width in longitude in the Northern Atlantic. The values of the width are $L = 20°$, $10°$ and $5°$, and the sections are taken in the window from 100° W to 40° W. (b) The same distributions under rescaling. Note that the rescaling is done with the mean value because although the power-law exponent is greater than one, the power-law behaviour is lost at small values of the *PDI*, see Subsec. 2.6.

Figure S7(a) shows the results of this procedure applied to the North Atlantic for regions of different width in longitude. It is apparent how the tail of the distribution moves to the left while keeps its shape nearly constant when the size of the region is decreased. The rescaling of the densities with their mean values yields the collapse of the distributions, which is shown in Fig. S7(b). Similar results hold for the other basins.

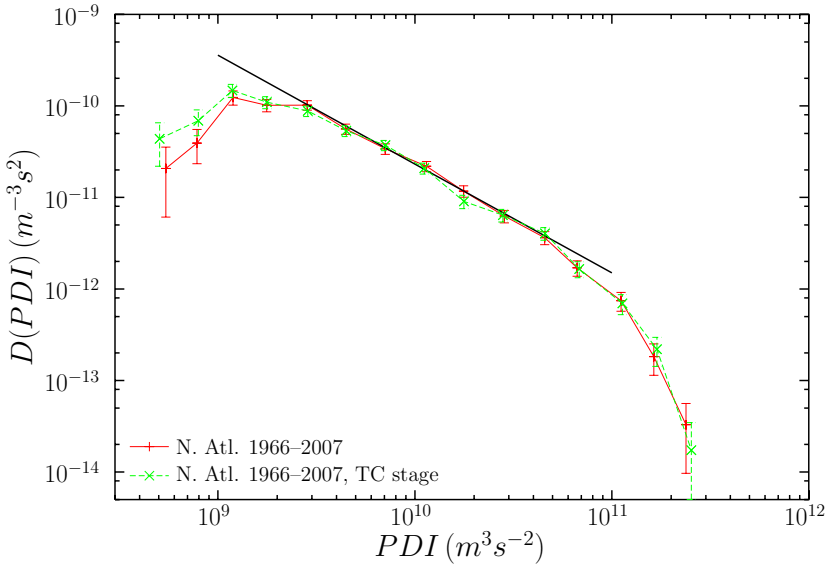

FIGURE 8. *PDI* probability density for Northern Atlantic tropical cyclones when the stage of the storm is strictly that corresponding to a tropical cyclone, and the same density when this restriction is released (as in the main text).

2.4. **Robustness of Results.** First, we check the robustness of the distribution over long periods of time. For the two distributions in Fig. 1(b), corresponding to N. Atlantic hurricanes for the years 1900-1953 and 1954-2007, the estimated power-law exponents and $p-$values are displayed in the bottom part of Table S1, showing a good agreement between them and with the more reliable period 1966-2007. Moreover, the two-sample KS test described in the previous section yields a value $d = 0.07$, which leads to $p = 15\%$. If we fix a minimum value *PDI* value $A = 2 \cdot 10^9 \mathrm{m}^3/\mathrm{s}^2$ then $d = 0.055$, and $p = 51\%$. (Comparison of 1954-2007 with the subset 1966-2007 yields a $p-$value around 97 %.) We conclude then that the distributions for the two periods cannot be considered as different.

In order to test further the robustness of our results, we introduce variations in the definition of the *PDI* of a storm. Figure S8 shows the *PDI* distribution for the North Atlantic when extratropical, subtropical, wave and low stages are not accounted in the

calculation of the *PDI*. If US landfalling hurricanes are excluded from the North Atlantic record, the *PDI* distribution is that appearing in Fig. S9. No essential difference arises between these distributions and those appearing in the main text, included also here for comparison.

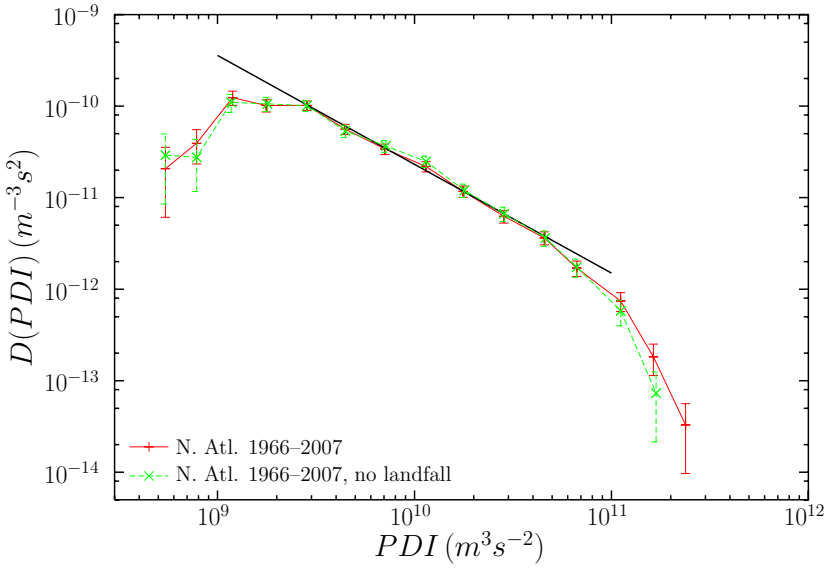

FIGURE 9. *PDI* probability density for Northern Atlantic tropical cyclones excluding those that make landfall in the US. The original distribution is also shown.

It has been suggested that the measurement of wind velocities previous to 1970 was not well calibrated. Following an approach by Landsea, we correct those velocities simply by subtracting 4 m/s [16]. This correction changes significantly small values of the *PDI*, but not the rest of values, and in this way the shape of the *PDI* distribution keeps very similar, except at small values, as can be seen in Fig. S10. Nevertheless, Landsea has later argued that the correction is probably not necessary [17].

Finally, other estimations of tropical cyclone dissipation, apart from *PDI*, have been suggested. It is remarkable the so called accumulated cyclone energy (*ACE*), defined as

$$ACE = \sum_t v_t^2 \Delta t,$$

which is related to the kinetic energy [18]. Note that the essential difference with *PDI* is the replacement of the cube of the velocity by its second power. Our conclusions do not change if we replace *PDI* by *ACE*, in particular, the values of the exponents are nearly the same. The reason is that *PDI* and *ACE* are highly correlated, and we can consider that a functional dependence exists between both variables. As the power-law exponents are very close to one, a change of variables from *PDI* to *ACE* changes very little the value of the exponents.

CRM Preprint Series number 1073

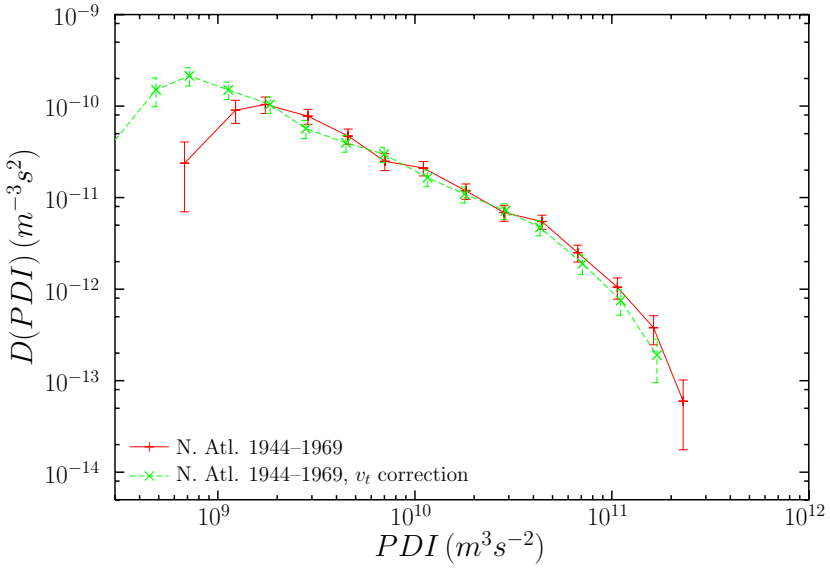

FIGURE 10. *PDI* probability density for Northern Atlantic tropical cyclones when the wind velocity is corrected as $v_t \to v_t - 4$ m/s. The original distribution is also shown.

2.5. **Invariance of Power-Law Distributions under Random Partitions.** Let us consider a random variable x, distributed according to the density $D(x)$. For each x, we will generate a uniform random number u between 0 and x, so that $x = u + (x-u)$. So, given an $x-$value, the distribution of u conditioned to the value of x can be written as

$$D(u|x) = \frac{\theta(x-u)}{x} \equiv \begin{cases} 1/x & \text{for } 0 \le u < x \\ 0 & \text{for } u > x \end{cases},$$

where θ is the Heaviside step function. This process represents the split of a tropical cyclone into two smaller ones, due to incomplete historical observations. We will obtain the distribution of u, $D(u)$, which plays the role of the observed *PDI*, as a function of that of x, the "true" *PDI*. (In fact, one should also take into account the distribution of $x-u$, but in virtue of the symmetry of the uniform distribution u and $x-u$ are distributed in the same way). From the total probability theorem, marginalization of the joint density $D(x,u)$ yields $D(u)$,

$$D(u) = \int_{\forall x} D(x,u)dx = \int_{\forall x} D(u|x)D(x)dx = \int_u^\infty \frac{D(x)}{x}dx.$$

Substituting in this equation a power-law distribution for x, $D(x) = C/x^\alpha$, it is easy to get that u turns power-law distributed as well, with the same exponent:

$$D(u) = \int_u^\infty \frac{C}{x^{1+\alpha}}dx = \frac{C}{\alpha u^\alpha}.$$

If not all the tropical cyclones undergo this split process, the observed distribution will be a statistical mixture of $D(x)$ and $D(u)$, which obviously will be a power law with the same exponent α.

The argument can be easily generalized for the case in which x is power-law distributed only in a certain range of values. In conclusion, if power-law distributed tropical cyclones are broken randomly into two parts, the resulting distribution turns out to be also a power law with the same exponent.

2.6. **Scaling of Distributions with exponent larger than one .** Let us assume that the probability density of a certain quantity s depends on a parameter a through a scaling form, i.e.,

$$D(s,a) = a^{-\beta} g(s/a^{\nu}),$$

where ν and β are scaling exponents and $g(s/a^{\nu})$ is a scaling function. (We will assume that $\nu > 0$.) If the distribution is defined between s_{min} and ∞, the kth order moment of the distribution is, by definition,

$$\langle s^k \rangle \equiv \int_{s_{min}}^{\infty} s^k D(s,a) ds$$

and in principle depends on a. Using the scaling ansatz and the change of variable $s/a^{\nu} = x$, the kth moment can be written as

$$\langle s^k \rangle = a^{(k+1)\nu-\beta} \int_{s_{min}/a^{\nu}}^{\infty} x^k g(x) dx. \tag{1}$$

We are interested in two different cases in the limit of small s (we assume that in the limit of large s the integral converges):

- Case 1. In the limit of small s we have $D(s,a) \sim C/s^{\alpha}$, with $\alpha < 1$. Then the integral of $x^k g(x)$ converges when $x \to 0$ and we will have $\langle s^k \rangle \sim a^{(k+1)\nu-\beta}$. Applying that the zero order moment is one (by normalization), we find that

  $$\beta = \nu$$

  and from here,

  $$\langle s^k \rangle \sim a^{k\nu}.$$

  In particular, $\langle s \rangle \sim a^{\nu}$, and substituting in the scaling ansatz

  $$D(s, \langle s \rangle) = g(s/\langle s \rangle)/\langle s \rangle;$$

  in words, the distribution scales with its mean value.
- Case 2. In the limit of small s we have $D(s,a) \sim C/s^{\alpha}$, with $\alpha > 1$. Then, for $\alpha > k+1$, the integral of $x^k g(x)$ diverges when $x \to 0$ as $a^{\nu(\alpha-k-1)}$. For $k = 0$ we get $1 \sim a^{\nu\alpha-\beta}$. So, the normalization condition implies that

  $$\beta = \nu\alpha$$

  Turning back to $\langle s^k \rangle$ we can write

  $$\langle s^k \rangle = \text{ constant if } k+1 < \alpha.$$

Increasing the value of k, the integral in Eq. (1) converges and we are in the first case, which gives now

$$\langle s^k \rangle \sim a^{\nu(k+1-\alpha)} \text{ if } k+1 > \alpha.$$

In the case of the *PDI* of tropical cyclones, $\alpha < 2$, and the previous equation is already valid for $k = 1$. In this way, the mean scales with a as $\langle s \rangle \sim a^{\nu(2-\alpha)}$. Substituting in the scaling ansatz,

$$D(s, \langle s \rangle) = g(s/\langle s \rangle^{1/(2-\alpha)})/\langle s \rangle^{\alpha/(2-\alpha)};$$

so, the distribution does not scale linearly with its mean, but with a power of its mean.

2.7. **Separation by *SST*, *MEI*, and high and low activity.** As described in the main text, in order to investigate the effect of sea surface temperature and El Niño on the dissipation of individual tropical cyclones, we separate the *PDI* data into years of high and low *SST*, and into positive and negative *MEI*. The list of years we have obtained in each case in each one of the basins studied appears in Table S2. For these restricted data sets, the estimated power-law exponents and the $p-$ values quantifying the goodness of the fits, as well as other related quantities, are shown in Table S3. In all cases the power-law hypothesis is acceptable, being the worst one that of the N. Atlantic in years of low *SST*, for which we have obtained $p = 9\%$. Nevertheless, remember that the $p-$value has to be uniformly distributed between 0 and 1, and as we are testing about 20 data sets it is possible that some of them yields p even below 5%, in the case in which the data were indeed power-law distributed. In the N. Atlantic and E. Pacific we also notice some systematic decrease in the value of the exponent when going from low activity (low *SST* or $MEI < 0$) to high activity; in some cases this decrease is small (below 0.15) but in some others can be about 0.25.

2.8. **Separation by *SST*, *MEI*, and high and low activity.** As described in the main text, in order to investigate the effect of sea surface temperature and El Niño on the dissipation of individual tropical cyclones, we separate the *PDI* data into years of high and low *SST*, and into positive and negative *MEI*. The list of years we have obtained in each case in each one of the basins studied appears in Table S2. For these restricted data sets, the estimated power-law exponents and the $p-$ values quantifying the goodness of the fits, as well as other related quantities, are shown in Table S3. In all cases the power-law hypothesis is acceptable, being the worst one that of the N. Atlantic in years of low *SST*, for which we have obtained $p = 9\%$. Nevertheless, remember that the $p-$value has to be uniformly distributed between 0 and 1, and as we are testing about 20 data sets it is possible that some of them yields p even below 5%, in the case in which the data were indeed power-law distributed. In the N. Atlantic and E. Pacific we also notice some systematic decrease in the value of the exponent when going from low activity (low *SST* or $MEI < 0$) to high activity; in some cases this decrease is small (below 0.15) but in some others can be about 0.25.

N. Atl. high SST:
1966 1969 1979 1980 1981 1983 1987 1990 1995 1997 1998 1999 2001 2002 2003 2004 2005 2006 2007
N. Atl. low SST:
1967 1968 1970 1971 1972 1973 1974 1975 1976 1977 1978 1982 1984 1985 1986 1988 1989 1991 1992 1993 1994 1996 2000
E. Pac. high SST:
1972 1976 1982 1983 1986 1987 1990 1991 1992 1993 1994 1995 1996 1997 1998 2001 2002 2003 2004 2005 2006
E. Pac. low SST:
1966 1967 1968 1969 1970 1971 1973 1974 1975 1977 1978 1979 1980 1981 1984 1985 1988 1989 1999 2000 2007
E. Pac. $MEI > 0$:
1966 1969 1972 1977 1978 1979 1980 1981 1982 1983 1986 1987 1990 1991 1992 1993 1994 1995 1997 1998 2002 2003 2004 2005 2006
E. Pac. $MEI < 0$:
1967 1968 1970 1971 1973 1974 1975 1976 1984 1985 1988 1989 1996 1999 2000 2001 2007
W. Pac. $MEI > 0$:
1986 1987 1990 1991 1992 1993 1994 1995 1997 1998 2002 2003 2004 2005 2006
W. Pac. $MEI < 0$:
1988 1989 1996 1999 2000 2001 2007

TABLE 2. Separation of the years as a function of the value of SST and MEI.

Additionally, we can apply a two-sample Kolmogorov-Smirnov test to each pair of high/low SST, or positive/negative MEI (those appearing in Fig. 2(a)) in order to quantify the difference between them. We summarize the results here. For the N. Atl, when years are separated by SST we get: $d = 0.10$, $p = 22\%$; for the E. Pac, separating by SST: $d = 0.13$, $p = 1\%$; for the E. Pac, separating by MEI: $d = 0.10$, $p = 7\%$; and for the W. Pac, separating by MEI: $d = 0.11$, $p = 8\%$. Except for the N. Atlantic, the $p-$values are rather low, indicating that it is unlikely that the distributions are the same.

However, if we rescale the PDIs, in the way already explained and displayed in Fig. 2(b) (i.e., dividing by $\langle PDI\rangle^{\nu}$), the KS distances decrease and the $p-$values increase. Nevertheless, the $p-$values obtained in this case are not reliable, as the rescaling parameter in each case has been calculated from the same data set, introducing a bias. Anyhow, as an indication, we report the obtained results for the KS statistic, $d = 0.055, 0.052, 0.052$ and 0.038 for $PDI/\langle PDI\rangle^{\nu} > 0.0003$, 0.0005, 0.0005 and 0, in units of $(m^3/s^2)^{1-\nu}$ (reported in the same order as above); for curiosity, the biased $p-$values are 90 %, 80 %, 81 % and 99%.

Finally, the N. Atlantic high-activity periods displayed in Fig. 3, are compared by means of a two-sample KS test too. The results are summarized in Table S4, showing that these distributions are highly compatible between them, but much less compatible with the one for the quiet period 1970-1994.

Basin	N	$A\,(\mathrm{m}^3/\mathrm{s}^2)$	$B\,(\mathrm{m}^3/\mathrm{s}^2)$	N_{AB}	CN_{AB}/N	$\alpha \pm \sigma_\alpha$	d_{data}	$p-$value
N. Atl. 1966-2007 *SST* ↑	250	$2.7 \cdot 10^9$	$7.4 \cdot 10^{10}$	175	8.216	1.13 ± 0.08	$2.82 \cdot 10^{-2}$	79 ± 4 %
N. Atl. 1966-2007 *SST* ↓	219	$2.2 \cdot 10^9$	$7.4 \cdot 10^{10}$	178	128.630	1.26 ± 0.07	$4.58 \cdot 10^{-2}$	$^*7 \pm 3$ %
E. Pac. 1966-2007 *SST* ↑	350	$1.6 \cdot 10^9$	$10.0 \cdot 10^{10}$	303	1.297	1.07 ± 0.05	$2.16 \cdot 10^{-2}$	86 ± 3 %
E. Pac. 1966-2007 *SST* ↓	324	$2.5 \cdot 10^9$	$5.8 \cdot 10^{10}$	228	61.571	1.21 ± 0.07	$3.64 \cdot 10^{-2}$	10 ± 3 %
E. Pac. 1966-2007 *MEI* ↑	400	$1.4 \cdot 10^9$	$6.3 \cdot 10^{10}$	325	0.802	1.04 ± 0.05	$1.93 \cdot 10^{-2}$	95 ± 2 %
E. Pac. 1966-2007 *MEI* ↓	274	$2.9 \cdot 10^9$	$8.6 \cdot 10^{10}$	197	571.587	1.31 ± 0.07	$3.06 \cdot 10^{-2}$	67 ± 5 %
W. Pac. 1986-2007 *MEI* ↑	404	$1.5 \cdot 10^9$	$6.8 \cdot 10^{10}$	289	0.097	0.94 ± 0.05	$2.28 \cdot 10^{-2}$	78 ± 4 %
W. Pac. 1986-2007 *MEI* ↓	188	$0.7 \cdot 10^9$	$9.3 \cdot 10^{10}$	175	0.036	0.92 ± 0.05	$3.64 \cdot 10^{-2}$	34 ± 5 %
N. Atl. 1926-1970	427	$1.6 \cdot 10^9$	$10.0 \cdot 10^{10}$	370	1.089	1.06 ± 0.04	$2.58 \cdot 10^{-2}$	40 ± 5 %
N. Atl. 1945-1970	257	$2.2 \cdot 10^9$	$7.9 \cdot 10^{10}$	198	0.565	1.02 ± 0.07	$2.45 \cdot 10^{-2}$	93 ± 3 %
N. Atl. 1945-1969	247	$1.3 \cdot 10^9$	$7.4 \cdot 10^{10}$	209	0.154	0.97 ± 0.06	$2.26 \cdot 10^{-2}$	99 ± 1 %
N. Atl. 1945-1969 corr	247	$0.5 \cdot 10^9$	$5.8 \cdot 10^{10}$	213	0.062	0.94 ± 0.05	$2.49 \cdot 10^{-2}$	93 ± 3 %
N. Atl. 1995-2005	166	$1.0 \cdot 10^9$	$9.3 \cdot 10^{10}$	147	0.276	1.00 ± 0.06	$2.87 \cdot 10^{-2}$	94 ± 2 %
N. Atl. 1945-1970, 1971-1994 *SST* ↑, 1995-2005	506	$2.2 \cdot 10^9$	$7.4 \cdot 10^{10}$	380	1.296	1.05 ± 0.05	$1.82 \cdot 10^{-2}$	92 ± 3 %
N. Atl. 1971-1994	222	$2.2 \cdot 10^9$	$7.4 \cdot 10^{10}$	181	145.935	1.26 ± 0.07	$3.62 \cdot 10^{-2}$	50 ± 5 %
W. Pac. 1986-2007 no TD	592	$1.0 \cdot 10^9$	$7.4 \cdot 10^{10}$	474	0.055	0.93 ± 0.04	$1.72 \cdot 10^{-2}$	92 ± 3 %

$^*9.0 \pm 0.9\%$ if $N_s = 1000$

TABLE 3. Parameters of the maximum likelihood estimation and the KS test for the *PDI* data in Figs. 2 and 3 (and other related data). The up arrow denotes a high or positive phase of *SST* and *MEI*, just the opposite as the down arrow. The $p-$value is calculated using $N_s = 100$ simulations. Tropical depressions have been removed in the W. Pac. record. The term *corr* refers to the subtraction of 4 m/s to all velocities [16].

2.9. **Distribution of 6-Hour Velocities.** Figure S11 shows the probability densities of the maximum sustained surface wind velocity (evaluated every 6 hours), $D(v_t)$, conditioned to *SST* above or below its mean or conditioned to $MEI > 0$ or $MEI < 0$. Note that these distributions are different to those calculated by Emanuel [19], who measured velocity in units of the potential intensity at each time.

	N	1945-1970	high SST, 1966-2007	1995-2005	1971-1994
1945-1970	257	–	36.4 %	44.4 %	0.2 %
high SST, 1966-2007	250	0.081	–	95.0 %	22.0 %
1995-2005	166	0.085	0.051	–	5.7 %
1971-1994	222	0.167	0.096	0.135	–

TABLE 4. KS distance d (below the diagonal) and $p-$value (above) for the results of the two sample KS test applied to the Atlantic hurricanes' PDI, for two different active periods, and for the years of high SST during 1966-2007, compared also to the low-activity period 1971-1994. Notice that the data set for high SST years between 1966 and 2007 is not independent of the rest.

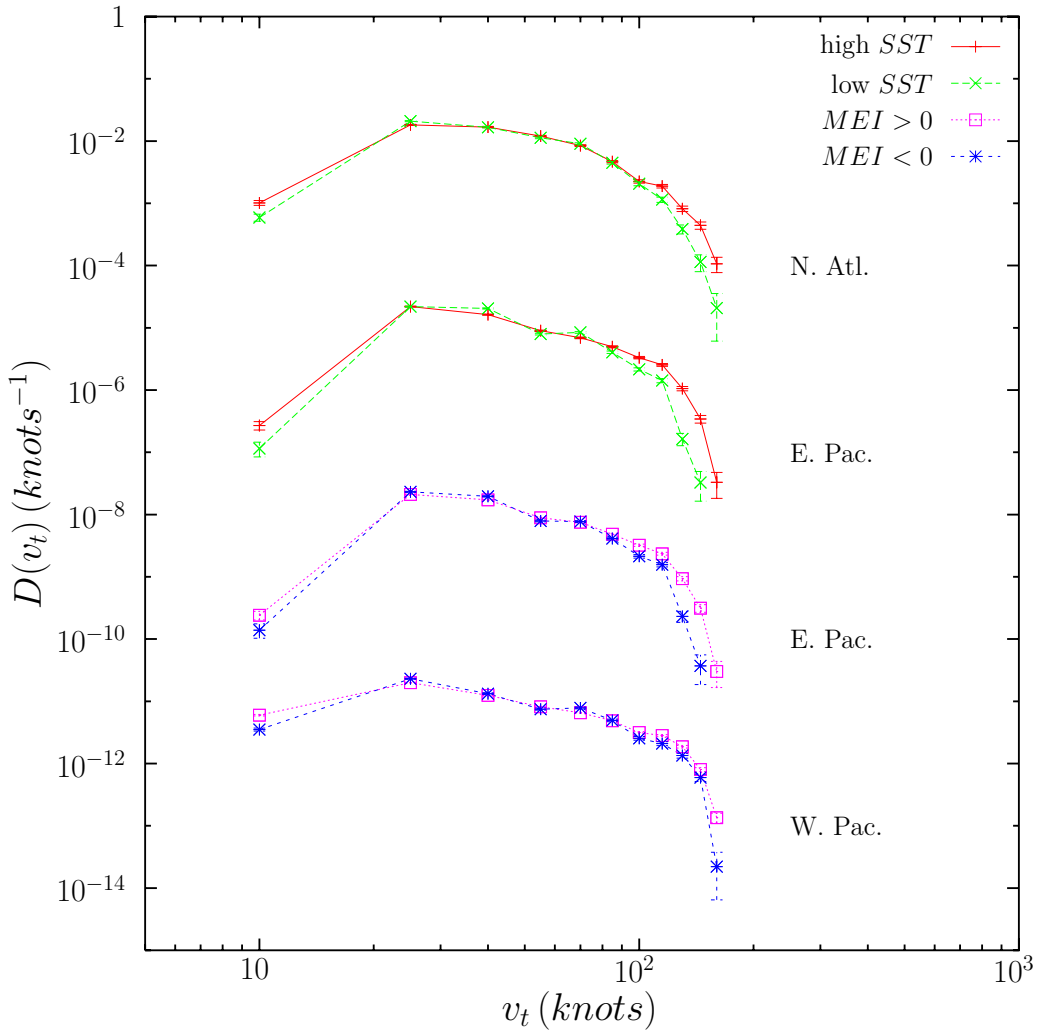

FIGURE 11. (a) Maximum sustained surface wind velocity probability densities $D(v_t)$ separated for high *SST* and low *SST* in the North Atlantic and Northeastern Pacific, and for $MEI > 0$ or $MEI < 0$, in the Northeastern Pacific and Northwestern Pacific (shifted in the vertical axis by integer powers of 1000 for clarity sake). Time periods are the same as in Figs. 1(a) and 2. We have used bins of constant size, equal to 15 knots, starting at 2.5 knots. The ratios of mean velocities between years of high and low *SST* or *MEI*, $\langle v_t \rangle_{high}/\langle v_t \rangle_{low}$, are 1.05, 1.07, 1.08 and 1.04, from top to bottom. When the average is for the cube of the velocity, we find $\langle v_t^3 \rangle_{high}/\langle v_t^3 \rangle_{low} = 1.25$, 1.4, 1.35 and 1.2. For comparison, the lifetimes of the TCs verify $\langle T \rangle_{high}/\langle T \rangle_{low} = 1.1$, 1.15, 1.05 and 1.2.

ACKNOWLEDGEMENTS

We are grateful to the University of Wisconsin – Cooperative Institute for Meteorological Satellite Studies for allowing us to use their images of hurricane Katrina at Fig. S1. Thanks also to A. González from the University of Zaragoza for his help with the maps.

REFERENCES

[1] B. R. Jarvinen, C. J. Neumann, and M. A. S. David. A tropical cyclone data tape for the North Atlantic basin, 1886-1983: contents, limitations, and uses. `http://www.nhc.noaa.gov/pdf/NWS-NHC-1988-22.pdf`, 1988.

[2] National Hurricane Center. `http://www.nhc.noaa.gov/tracks1851to2007$_$atl$_$reanal.txt,http://www.nhc.noaa.gov/tracks1949to2007$_$epa.txt`.

[3] J.-H. Chu, C. R. Sampson, A. S. Levine, and E. Fukada. The Joint Typhoon Warning Center tropical cyclone best-tracks, 1945-2000. *https://metocph.nmci.navy.mil/jtwc/best_tracks/TC_bt_report.html*, 2002.

[4] Joint Typhoon Warning Center. *https://metocph.nmci.navy.mil/jtwc/best_tracks/index.html*.

[5] S. Hergarten. *Self-Organized Criticality in Earth Systems*. Springer, Berlin, 2002.

[6] A. Corral. Dependence of earthquake recurrence times and independence of magnitudes on seismicity history. *Tectonophys.*, 424:177–193, 2006.

[7] A. Clauset, C. R. Shalizi, and M. E. J. Newman. Power-law distributions in empirical data. *SIAM Rev.*, 51:661–703, 2009.

[8] A. Corral. Statistical tests for scaling in the inter-event times of earthquakes in California. *Int. J. Mod. Phys. B*, 23:5570–5582, 2009.

[9] I. B. Aban, M. M. Meerschaert, and A. K. Panorska. Parameter estimation for the truncated Pareto distribution. *J. Am. Stat. Assoc.*, 101:270–277, 2006.

[10] W. H. Press, S. A. Teukolsky, W. T. Vetterling, and B. P. Flannery. *Numerical Recipes in FORTRAN*. Cambridge University Press, Cambridge, 2nd edition, 1992.

[11] E. Lippiello, L. de Arcangelis, and C. Godano. Influence of time and space correlations on earthquake magnitude. *Phys. Rev. Lett.*, 100:038501, 2008.

[12] S. Lennartz, V. N. Livina, A. Bunde, and S. Havlin. Long-term memory in earthquakes and the distribution of interoccurrence times. *Europhys. Lett.*, 81:69001, 2008.

[13] Hurricane Season Tropical Cyclone Reports. `http://www.nhc.noaa.gov/pastall.shtml#tcr`.

[14] JTWC Annual Tropical Cyclone Reports. `http://metocph.nmci.navy.mil/jtwc/atcr/atcr$_$archive.html`.

[15] Central Pacific Hurricane Center. `http://www.prh.noaa.gov/cphc/summaries`.

[16] C. W. Landsea. A climatology of intense (or major) hurricanes. *Mon. Weather Rev.*, 121:1703–1713, 1993.

[17] C. W. Landsea. Hurricanes and global warming. *Nature*, 438:E11–E12, 2005.

[18] G. D. Bell, M. S. Halpert, R. C. Schnell, R. W. Higgins, J. Lawrimore, V. E. Kousky, R. Tinker, W. Thiaw, M. Chelliah, and A. Artusa. Climate assessment for 1999. *Bull. Am. Met. Soc.*, 81(6):S1–S50, 2000.

[19] K. Emanuel. A statistical analysis of tropical cyclone intensity. *Mon. Wea. Rev.*, 128:1139–1152, 2000.

ÁLVARO CORRAL
CENTRE DE RECERCA MATEMÀTICA
EDIFICI CC, CAMPUS UNIVERSITARI
E-08193 BELLATERRA, BARCELONA, SPAIN
E-mail address: ACorral@crm.cat

ALBERT OSSÓ, JOSEP ENRIC LLEBOT
GRUP DE FÍSICA ESTADÍSTICA
FACULTAT DE CIÈNCIES
UNIVERSITAT AUTÒNOMA DE BARCELONA
E-08193 BELLATERRA, BARCELONA, SPAIN

CRM Preprint Series number 1073